PHYSICAL REVIEW E **76**, 010402(R) (2007)

Reversible clustering under the influence of a periodically modulated binding rate

Ronny Straube[*]
Max-Planck-Institute for Dynamics of Complex Technical Systems, Department of Systems Biology, Sandtorstrasse 1, D-39106 Magdeburg, Germany

Martin Falcke
Hahn-Meitner-Institute, Department of Theoretical Physics SF5, Glienicker Strasse 100, D-14109 Berlin, Germany

(Received 17 April 2007; published 26 July 2007)

We study cluster-cluster aggregation and fragmentation with a periodically modulated binding rate. Using the Smoluchowski mean-field equations, we derive exact solutions for the cluster size distribution for two time courses of the binding rate: (i) harmonic modulations and (ii) on-off switching of the binding rate with dwell times τ_b and τ_f. In both cases, the asymptotic cluster size distribution is oscillatory in time. The formation of small-sized clusters is enhanced compared to a constant binding rate below a critical cluster size s_c. There is another critical cluster size s_p close to which the size distribution becomes quasistationary. We calculate analytically the dependence of the critical points s_c and s_p on the relevant system parameters for on-off switching of the binding rate. Our results are relevant whenever clustering can be externally controlled.

DOI: 10.1103/PhysRevE.76.010402 PACS number(s): 61.43.Hv, 05.45.−a, 82.30.Nr, 82.40.Bj

We study reversible clustering which may be schematically represented as

$$N_i + N_j \underset{F_{ij}(t)}{\overset{K_{ij}(t)}{\rightleftarrows}} N_{i+j}. \qquad (1)$$

In general, the aggregation and fragmentation kernels K and F depend on cluster size and time. Cluster-size-dependent kernel functions have been extensively studied [1–3], and several scaling regimes of the cluster size distribution were identified [4–6]. However, time-dependent kernels received only little attention. In Ref. [7] the asymptotic cluster size distribution for monotonic time-dependent kernel functions has been investigated.

Recent experiments suggest that clustering can be externally controlled by changing the aggregation rate. In particular, it has been shown that cluster formation in ferrofluids can be reversibly induced by light [8]. Another example concerns the cluster formation of IP$_3$R ion channels on the membrane of the endoplasmic reticulum in living cells. The clustering of these ion channels requires the channel proteins to undergo a transition to the "open" state [9] which can be induced by the second messenger molecule IP$_3$. The open probability of the IP$_3$R channel is modulated periodically by oscillations of the intracellular Ca^{2+} concentration. Thus, one can expect that oscillations in the calcium concentration may lead to a temporal modulation of the binding affinity between IP$_3$R channels, thereby affecting its cluster size distribution.

Motivated by these observations, we investigate the influence of a periodically modulated aggregation rate on the asymptotic cluster size distribution for the most simple case where the aggregation kernel is a function of time only, $K_{ij}(t) \equiv k(t)$, and the fragmentation kernel is a simple constant, $F_{ij}(t) \equiv k_f$. It has been shown that the critical dimension of a system undergoing reversible aggregation is $d_c = 1$, meaning that spatial fluctuations will not influence the kinetic behavior of the system provided $d > d_c$ [4]. In this case a mean-field approach is appropriate and the dynamics of the kinetic scheme in Eq. (1) is governed by the set of equations for the number density n_s:

$$\frac{dn_s}{dt} = \frac{k(t)}{2}\sum_{i+j=s} n_i n_j - k(t) n_s \sum_{j=1}^{\infty} n_j - \frac{k_f}{2}\sum_{i+j=s} n_{i+j} + k_f \sum_{j=1}^{\infty} n_{s+j},$$

$$s = 1,2,\ldots . \qquad (2)$$

For the case of monodisperse initial conditions—i.e., $n_s(0) = n_0 \delta_{s1}$—the cluster size distribution corresponding to the infinite set of equations (2) is given by [7]

$$n_s(t) = n_0 [1 - n(t)]^2 [n(t)]^{s-1}, \quad s = 1,2,\ldots , \qquad (3)$$

where the function $n(t)$ solves the Ricatti equation

$$\dot{n}(t) = \frac{k(t) n_0}{2}[1 - n(t)]^2 - \frac{k_f}{2} n(t), \qquad (4)$$

with initial condition $n(0) = 0$. For convenience, the initial density of monomers n_0 will be set to 1. This gives $k(t)$ the same dimension $(1/s)$ as k_f.

In the following, we consider two cases for the aggregation kernel $k(t)$:

$$\text{(i)}\ k(t) = \frac{k_b}{2}\left[1 + \cos\left(\frac{2\pi}{T} t\right)\right], \qquad (5a)$$

$$\text{(ii)}\ k(t) = \begin{cases} k_b & t \in T_b^m, \\ 0 & t \in T_f^m, \end{cases} \qquad m = 0,1,2,\ldots . \qquad (5b)$$

k varies smoothly between zero and k_b with period T in Eq. (5a), while k equals k_b during the time interval T_b^m and remains zero during the subsequent interval T_f^m in Eq. (5b). The interval families T_b^m and T_f^m are defined in terms of "on"

---

[*] rstraube@mpi-magdeburg.mpg.de; URL: http://www.mpi-magdeburg.mpg.de/people/rstraube/index.html

1539-3755/2007/76(1)/010402(4)

and "off" time intervals τ_b and τ_f, respectively, as $(m=0,1,2,\ldots)$

$$T_b^m := \{t{:}m(\tau_b+\tau_f) \leqslant t \leqslant (m+1)\tau_b + m\tau_f\},$$

$$T_f^m := \{t{:}(m+1)\tau_b + m\tau_f \leqslant t \leqslant (m+1)(\tau_b+\tau_f)\}. \tag{6}$$

It can be expected that the two rate functions in Eqs. (5) yield qualitatively similar results for the cluster size distribution if $\tau_b=\tau_f$ and $\tau_b+\tau_f=T$ hold.

We derive explicit solutions of the Ricatti equation for the two cases corresponding to Eqs. (5a) and (5b). In the first case, the Ricatti equation (4) is transformed to the system of linear differential equations $(n_0=1)$

$$\dot{\alpha} = -\left(k(t) + \frac{k_f}{4}\right)\beta, \tag{7a}$$

$$\dot{\beta} = -\frac{k_f}{4}\alpha, \tag{7b}$$

where the functions $\alpha(t)$ and $\beta(t)$ are related to the original function $n(t)$ by the nonlinear transformation [10]

$$n(t) = \frac{\alpha(t)+\beta(t)}{\alpha(t)-\beta(t)}. \tag{8}$$

Upon inserting the expression for $k(t)$ from Eq. (5a) into Eq. (7a), it is straightforward to see that Eqs. (7) are equivalent to the Mathieu equation

$$\ddot{\beta}(t) = \left[\frac{k_f}{4}\left(\frac{k_b}{2}+\frac{k_f}{4}\right) + \frac{k_b k_f}{8}\cos\left(\frac{2\pi}{T}t\right)\right]\beta(t). \tag{9}$$

A comparison with the canonical form of the Mathieu equation $y''(\tau)+(a-2q\cos 2\tau)y(\tau)=0$ yields that, if we set $\tau=\pi t/T$, the parameters a and q are given by $a \equiv -T^2 k_f(2k_b+k_f)/16\pi^2$ and $q \equiv T^2 k_b k_f/16\pi^2$, respectively. The initial condition for $\beta(t)$ in Eq. (9) can be arbitrarily fixed at $\beta(0)=1$. In addition, we must require that $n(0)=0$. Using Eq. (8) yields that $n(0)=0=\alpha(0)+\beta(0) = -\frac{4}{k_f}\dot{\beta}(0)+\beta(0)$ which shows that $\dot{\beta}(0)=k_f/4$ must be fulfilled.

The Mathieu equation (9) has periodic solutions only for particular values $a(q)$ for given values of q [11]. In our case, the parameters a and q are given in terms of the intrinsic system parameters k_b, k_f, and T. Therefore, in general, we cannot expect the solution of Eq. (9) to be periodic. However, since the function $n(t)$ which enters the cluster size distribution, Eq. (3), depends on the ratio of Mathieu functions only and their first derivative [cf. Eq. (8)], it can be shown that $n(t)$ is always asymptotically periodic independent of the particular values of a and q.

In the case of on-off switching, Eq. (5b), the Ricatti equation (4) has to be solved in each of the intervals T_b^m and T_f^m [cf. Eqs. (6)] separately—i.e., $(n_0=1)$,

$$\dot{a}_m(t) = \frac{k_b}{2}[1-a_m(t)]^2 - \frac{k_f}{2}a_m(t), \quad t \in T_b^m,$$

$$\dot{b}_m(t) = -\frac{k_f}{2}b_m(t), \quad t \in T_f^m, \quad m=0,1,2,\ldots .$$

Since both k_b and k_f are constant, the solutions of these equations in their respective intervals are simply

$$a_m(t) = B - \frac{D}{2K}\coth\left(\frac{k_f D}{4}t + C_m\right), \quad t \in T_b^m,$$

$$b_m(t) = A_m \exp\left(-\frac{k_f}{2}t\right), \quad t \in T_f^m, \tag{10}$$

with $m=0,1,2,\ldots$ and we have introduced the abbreviations $K=k_b/k_f$, $D=\sqrt{1+4K}$ and $B=1+1/2K$. When time is measured in units of $1/k_f$, there are only three free parameters describing the solution in Eqs. (10): $K=k_b/k_f$, τ_b, and τ_f.

The integration constants C_m and A_m in Eqs. (10) are determined by the initial condition $a_0(t=0)=0$ as well as by the requirement of continuity of the solutions a_m and b_m at the boundaries of the intervals T_b^m and T_f^m. The initial condition fixes C_0 as

$$C_0 = \coth^{-1}\frac{2K+1}{D}. \tag{11}$$

The requirement for continuity of the solutions, Eqs. (10), leads to the following recurrence equations for the integration constants C_m and A_m:

$$C_{m+1} = \coth^{-1}\left[\frac{2K}{D}(B - A_m e^{-(k_f/2)\tau_q})\right], \tag{12a}$$

$$A_m = B - \frac{D}{2K}\coth\left(\frac{k_f D}{4}\tau_b + C_m\right), \tag{12b}$$

with $m=0,1,2,\ldots$. Combining these two equations yields the closed recurrence equation $C_{m+1}=\coth^{-1}[F+E\coth(L+C_m)]$ with $m=0,1,2,\ldots$. The fixed point of this equation reads

$$C^0 = \coth^{-1}\left[G\left(1+\sqrt{1+\frac{F\coth(L)+E}{G^2}}\right)\right], \tag{13}$$

with $E=\exp(-k_f\tau_f/2)$, $F=(2KB/D)(1-E)$, $L=k_f D\tau_b/4$, and $G=[F-(1-E)\coth(L)]/2$. According to Eq. (12b) the value for A^0 is obtained from C^0 as

$$A^0 = B - \frac{D}{2K}\coth\left(\frac{k_f D}{4}\tau_b + C^0\right). \tag{14}$$

Our numerical investigations indicate that the fixed point is always stable in the region $K>1$ for any ratio τ_b/τ_f as long as $k_f\tau_f$ and $k_f\tau_b$ are bounded away from zero.

A stable fixed point of the recurrence equations (12) corresponds to an asymptotically periodic cluster size distribution of period $T=\tau_b+\tau_f$ given by

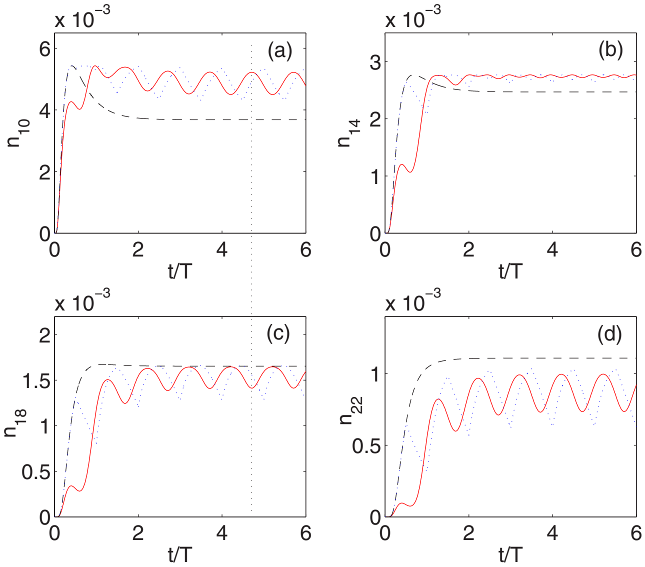

FIG. 1. (Color online) Temporal plot of the number density $n_s(t)$ [cf. Eq. (3)] for $s=10$ (a), $s=14$ (b), $s=18$ (c), and $s=22$ (d). Solid lines correspond to the solution of the Mathieu equation in Eq. (9) while dashed lines correspond to a constant binding rate $k\equiv k_b$. Dotted lines denote the solution for on-off switching corresponding to Eqs. (10). Parameters are $T=60$ s, $K=100$, $k_b=0.4/\mathrm{s}$, and $\tau_b=30\ \mathrm{s}=\tau_f$.

$$n_s(t)=\begin{cases}[1-a_m^0(t)]^2[a_m^0(t)]^{s-1}, & t\in T_b^m,\\ [1-b_m^0(t)]^2[b_m^0(t)]^{s-1}, & t\in T_f^m,\end{cases}\qquad m\gg 1. \tag{15}$$

The functions a_m^0 and b_m^0 are the same as in Eqs. (10). The only difference is that the integration constants C_m and A_m are now replaced by the fixed points C^0 [Eq. (13)] and A^0 [Eq. (14)], respectively.

The temporal evolution of the number density n_s for the periodically modulated binding rate in Eq. (5a) (solid line) is compared with that for a constant binding rate $k(t)\equiv k_b$ (dashed line) in Fig. 1. In the latter case, $n_s(t)=[1-a_0(t)]^2a_0(t)^{s-1}$ with $a_0(t)$ given by Eqs. (10) for $m=0$ and $b_0\equiv 0$. The number density n_s approaches the stationary value

$$n_s^\infty=(1-a_0^\infty)^2(a_0^\infty)^{s-1},\qquad a_0^\infty=B-\frac{D}{2K}. \tag{16}$$

Several points are of interest here. Figure 1(a) shows that there are asymptotically more 10-clusters in the system for the case of an oscillating binding rate than with a constant binding rate. Conversely, the number of 22-clusters is larger in the case of a constant binding rate [Fig. 1(d)]. Thus, there must be a critical cluster size s_c where the maximal value of the asymptotic oscillations in the number density equals the stationary value of the number density for a constant binding rate. For the parameter values used in Fig. 1, this transition occurs at $s_c\approx 18$ [Fig. 1(c)]. The formation of s-clusters is enhanced by an oscillatory binding rate below the transition point s_c, while it is suppressed above that point. The amplitude of oscillations in the number density exhibits a minimum such that n_{14} becomes quasistationary in time while it is still larger than in the case of a constant binding rate [Fig. 1(b)]. The quasistationary behavior is caused by a second transition at $s_p\approx 14$. That transition is related to a phase shift of π between the oscillations below and above s_p [see dotted line from Fig. 1(a) to Fig. 1(c)].

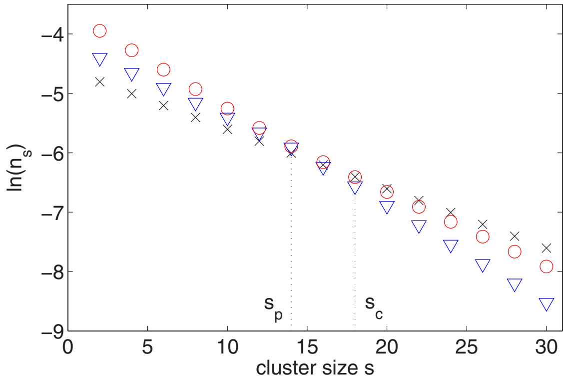

FIG. 2. (Color online) Asymptotic cluster size distribution for the parameters used in Fig. 1. Circles (○) and triangles (▽) denote maximum n_s^{max} and minimum n_s^{min} of the asymptotic oscillations (solid lines) in Fig. 1, respectively. The circles below s_p and the triangles above s_p are on a straight line. The same holds for the triangles below s_p and the circles above that point. Crosses (×) denote the stationary value n_s^∞ for the case of a constant binding rate. $s_p=14$ and $s_c=18$.

Both transitions are summarized in Fig. 2 which shows the asymptotic cluster size distribution for the case of an oscillatory binding rate according to Eq. (5a) and a constant binding rate. In the oscillatory case maxima (n_s^{max}) and minima (n_s^{min}) of the asymptotic oscillations in Fig. 1 are plotted as circles and triangles, respectively, while stationary values n_s^∞ in the case of constant binding rate are plotted as crosses. From Fig. 2 it is evident that n_s^{max}, n_s^{min}, and n_s^∞ decrease exponentially with cluster size s, but with different rates. Moreover, n_s^{max} and n_s^{min} exchange their decay behavior at s_p. Below s_p we have $n_s^{max}\sim\exp(-l_us)$ and $n_s^{min}\sim\exp(-l_ds)$ with $l_u>l_d>0$ while above s_p there is an exchange of decay rates between n_s^{max} and n_s^{min} where $n_s^{max}\sim\exp(-l_ds)$ and $n_s^{min}\sim\exp(-l_us)$ hold. The minima and maxima of the oscillations below the transition point turn into maxima and minima above the transition point s_p. This explains the phase shift of π shown in Figs. 1(a) and 1(c).

To determine the transition points s_p and s_c explicitly, it is advantageous to use the representation of the asymptotic cluster size distribution in Eq. (15) for the case of sharp on-off switching of the binding rate according to Eq. (5b). This solution is qualitatively the same as in the case of a harmonically modulated binding rate in Eq. (5a) provided $\tau_b=\tau_f$ and $\tau_b+\tau_f=T$ is chosen (compare dotted and solid lines in Fig. 1). The only difference is that the amplitude of the asymptotic oscillations is larger in the case of sharp on-off switching and there is a global phase shift between the two solutions. However, Eq. (15) also allows one to study different ratios of τ_b and τ_f which might be of relevance in experiments. During one period $T=\tau_b+\tau_f$ of the asymptotic

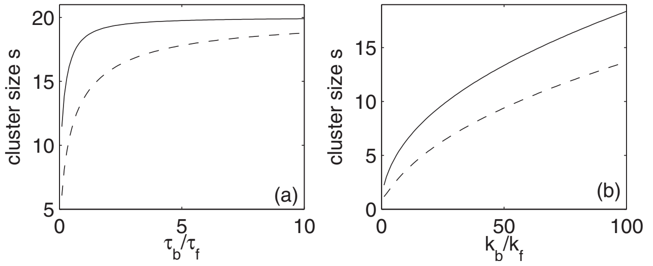

FIG. 3. Dependence of the transition points s_c (solid line) and s_p (dashed line) on the ratios $0.1 \leqslant \tau_b/\tau_f \leqslant 10$ (a) and $1 \leqslant k_b/k_f \leqslant 100$ (b). Parameters are $T=60$ s, $k_b=0.4/\text{s}$, $k_b/k_f=100$ (a), and $\tau_b/\tau_f=1$ (b).

oscillations in Eq. (15), a_m^0 rises to its maximal value in time τ_b given by $a_{max}^0=A^0$ [cf. Eq. (14)], and subsequently b_m^0 decreases exponentially according to the second equation in Eqs. (10) to its minimal value $b_{min}^0=A^0\exp(-k_f\tau_f/2)$ $=a_{max}^0\exp(-k_f\tau_f/2)$ in time, τ_f. The transition point s_p where the amplitude of $n_s(t)$, as given in Eq. (15), becomes quasistationary during subsequent time intervals T_b^m/T_f^m is determined by $(1-a_{max}^0)^2(a_{max}^0)^{s_p-1}=(1-b_{min}^0)^2(b_{min}^0)^{s_p-1}$. Likewise, the cluster size s_c where the asymptotic cluster number with stationary binding rate starts to exceed the maximum of the oscillations is determined by $(1-a_{max}^0)^2(a_{max}^0)^{s_c-1}$ $=(1-a_0^\infty)^2(a_0^\infty)^{s_c-1}$. The solution of these equations is given by

$$s_p = 1 + \frac{4}{\tau_f k_f}\ln\left(\frac{1-b_{min}^0}{1-a_{max}^0}\right), \tag{17a}$$

$$s_c = 1 + 2\ln\left(\frac{1-a_0^\infty}{1-a_{max}^0}\right)\bigg/\ln\left(\frac{a_{max}^0}{a_0^\infty}\right), \tag{17b}$$

where the nearest integer part has to be taken to obtain the critical cluster sizes. Figure 3 shows how the transition points s_p (dashed line) and s_c (solid line) depend on the ratio between the dwell times for on-off switching, τ_b/τ_f (a), and the ratio between the binding and fragmentation rate, k_b/k_f (b). The overall oscillation period of the binding rate is fixed at $T=60$ s.

To summarize, we studied reversible clustering with a periodically modulated binding rate. The periodic modulation always leads asymptotically to an oscillating cluster size distribution which contains a higher number of small sized clusters below a critical cluster size s_c as compared to the case of a constant binding rate. The period of the asymptotic oscillations is the same as the period of the modulation of the binding rate. It is known that in the case of constant aggregation and fragmentation kernels the cluster size distribution decays exponentially. We have shown that the same also holds for the maxima and minima of the asymptotic oscillations in the case of an oscillatory binding rate. However, the maxima and minima exchange their decay rates at another critical cluster size s_p where the amplitude of cluster size oscillations vanishes and the number density n_{s_p} is stationary. The oscillations above and below s_p are phase shifted by π.

Coming back to the experiment where reversible clustering could be induced by light [8] our results suggest that by applying light pulses of the right period and ratio τ_b/τ_f one may generate cluster size distributions with a larger number of small-sized clusters as compared to a constant illumination or stabilize the formation of a particular cluster size close to s_p which would then remain stationary in time.

---

[1] M. v. Smoluchowski, Z. Phys. Chem. **92**, 129 (1917).
[2] J. Ke and Z. Lin, Phys. Rev. E **66**, 050102(R) (2002).
[3] J. M. Ball and J. Carr, J. Stat. Phys. **61**, 203 (1990).
[4] F. Family, P. Meakin, and J. M. Deutch, Phys. Rev. Lett. **57**, 727 (1986).
[5] C. M. Sorensen, H. X. Zhang, and T. W. Taylor, Phys. Rev. Lett. **59**, 363 (1987).
[6] P. Meakin and M. H. Ernst, Phys. Rev. Lett. **60**, 2503 (1988).
[7] J. Ke, X.-O. Cai, and Z. Lin, Phys. Lett. A **331**, 281 (2004).
[8] R. R. Kellner and W. Köhler, J. Appl. Phys. **97**, 034910 (2005).
[9] Y. Tateishi, M. Hattori, T. Nakayama, M. Iwai, H. Bannai, T. Nakamura, T. Michikawa, T. Inoue, and K. Mikoshiba, J. Biol. Chem. **280**, 6816 (2005).
[10] H. Stephani, *Differentialgleichungen: Symmetrien und Lösungsmethoden* (Spektrum Akademischer Verlag, Heidelberg, 1994).
[11] *Handbook of Mathematical Functions*, edited by M. Abramowitz and I. A. Stegun (Dover, New York, 1964).